A MODIFIED HICUM MODEL FOR GaInP/GaAs HBT DEVICES

S.-C. Tseng, C. C. Meng, W.-Y. Chen, and J.-Y. Su
Department of Communications Engineering
National Chiao Tung University
Hsinchu, 300 Taiwan, R.O.C.

Received 20 October 2005

ABSTRACT: *A compact physics-based transit-time model is established for the GaInP/GaAs HBT device. The VBIC model fails to describe the transit-time frequency versus bias (I_C, V_{CE}), especially at low- and medium-current regimes. Starting with the HICUM model, we introduce a new time constant to describe the transit-time frequency versus bias (I_C, V_{CE}) more precisely. This model has obvious advantages over the VBIC model for showing the relation of* f_t *versus bias (I_C, V_{CE}) in the low and medium current regimes for GaInP/GaAs HBT devices.* © 2006 Wiley Periodicals, Inc. Microwave Opt Technol Lett 48: 780–783, 2006; Published online in Wiley InterScience (www.interscience.wiley.com). DOI 10.1002/mop.21474

Key words: *transit time; GaInP/GaAs HBT; minority charge; HICUM and VBIC*

1. INTRODUCTION

A good device model is important for circuit designers to perform accurate simulations. In recent years, using the HBT technology in radio-frequency integrated circuits has become popular. There are many proposed models such as the SPICE Gummel–Poon model (SGPM), VBIC [1], and HICUM [2]. However, the SGPM is not suitable for modern devices to design high-frequency integrated circuits because of the lack of (i) parasitic transistors, (ii) avalanche multiplication, (iii) self-heating, and (iv) quasi-saturation effects. Although the VBIC model is an advanced version of the SGP model, the transit-time frequency is not also accurately described when the VBIC is applied to the GaInP/GaAs HBT device. The HICUM model has the physics-based description for high-current effects, but it is still not perfectly matched to our GaInP/GaAs HBT device. Most of the models developed are made for BJT, not for GaInP/GaAs HBT. For example, the heavily doped base in HBT nullifies the base-width modulation and results in a very high early voltage. Some parts of the model should be modified to adapt itself to the GaInP/GaAs HBT device.

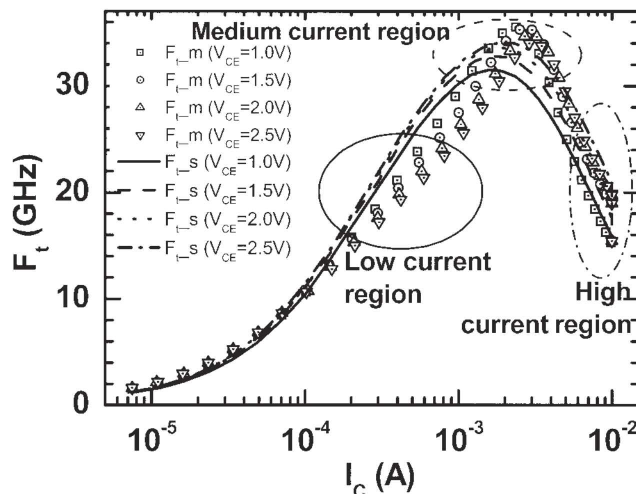

Figure 1 Measured transit-time frequency vs. collector current for various V_{CE} values and the fitting curves of the VBIC model

TABLE 1 Parameter Values of the VBIC Transient-Time Model

Parameter	Value	Parameter	Value
TF [psec]	3.012	ITF	20.61m
QTF	0	VTF	20
XTF	14.48	TR	0

In a VBIC model, the transit time is described as

$$TFF = TF \times (1 + QTF \times q_1) \times \left(1 + XTF \times \left(\frac{I_{tzf}}{I_{tzf} + ITF}\right)^2 e^{[V_{bci}/(1.44\times VTF)]}\right) = \frac{1}{2\pi f_T}. \quad (1)$$

It is a semi-physics model with five fitting parameters. TF is the ideal forward transit time, XTF is the coefficient of base push-out, QTF is the coefficient of base width modulation, ITF is the parameter for the onset of the collector high-current effects, and VTF is used to describe the effect of V_{BC} on the collector high-current effects. The curve fitting for transit-time frequency versus bias is shown in Figure 1. The values of the parameters from curve fitting are also shown in Table 1.

In Figure 1, it is obvious that (i) the modeled f_t in the low-current region is higher than the actual measured data, and (ii) there is a discrepancy for the dependence between f_t and V_{CE}. Measured f_t becomes lower for increasing V_{CE}. This phenomenon is very common in GaInP/GaAs HBTs. On the contrary, the VBIC model gives the opposite dependence between f_t and V_{CE}.

In a BJT, the transit time is dominated by the base transit time. The base transit time caused by the electron minority carriers in the base for the GaInP/GaAs HBT device is reduced drastically because GaAs has high electron mobility. Moreover, the base width becomes thinner such that the other transit time, for example, the BC SCR (base-collector space charge region) transit time becomes more important. Furthermore, in Eq. (1), the VBIC model does not describe well the dependence between f_t and V_{CE}. Thus, this model is not precise for GaInP/GaAs HBT technology.

An accurate transit-time model is indispensable for designing high-frequency circuits [3]. In this paper, we focus on the accurate descriptions of the transit-time frequency. Starting from a basic transit-time model [4], we introduce a new time constant and use fitting optimization to obtain the values of the circuit parameters. The simulated transit-time frequency versus bias (I_C, V_{CE}) shows excellent agreement with the measured data. The modified HICUM model suitable for the GaInP/GaAs HBT is demonstrated for the first time to the best of the authors' knowledge.

Section 2 gives a brief description of the transit-time model while section 3 represents the compact-model equation for the transit-time frequency. Finally, the agreement between the measured data and modeled curves is shown in section 4.

2. TRANSIT TIME MODELING

The transit-time constant in each region is derived for five regions of a device, as shown in Figure 2. The transit-time equations are obtained from the minority charge:

$$\tau = \frac{dQ}{dI}. \quad (2)$$

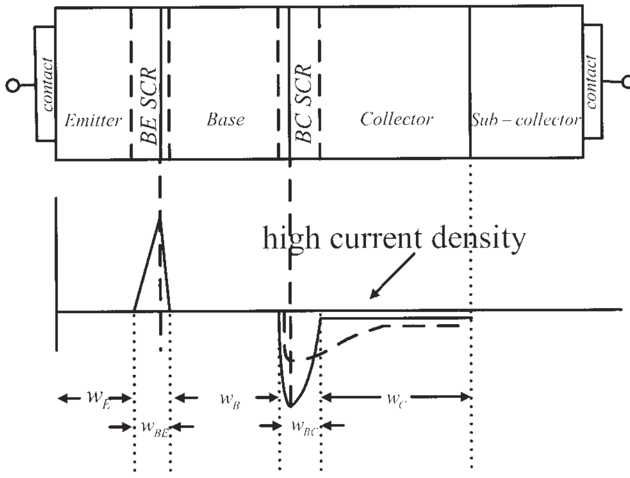

Figure 2 Five regions in a GaInP/GaAs HBT device

Here, the five regions are the neutral emitter region, base-emitter space charge region, neutral base region, base-collector space charge region, and neutral collector region.

2.1. Neutral Emitter Region

In this region, electron storage time converted from hole storage time is written as

$$\begin{cases} \tau_{Ef} = \tau_{Ef0}\left[1 + \left(\dfrac{I_T}{I_{CK}}\right)^{g_{\tau E}}\right] \\ \tau_{Ef0} = \dfrac{dQ_{pE}}{dI_C} = \dfrac{\dfrac{w_E^2}{v_{kE}} + \dfrac{w_E^2}{2\mu_{pE}V_T}}{\beta_0(I_{C,\mathrm{low}}, V_{BCi} = 0)} \end{cases}, \tag{3}$$

where Q_{pE} is the stored hole charge, w_E is the neutral emitter width, v_{kE} is the finite effective contact recombination velocity, μ_{pE} is the hole mobility, V_T is the thermal voltage, $g_{\tau E}$ is the model parameter, and I_{CK} is the critical current characterizing the onset of high-current effects in the collector.

In our study, $g_{\tau E} = 2.7$. Thus, electron storage time is strong in relation to the transfer current I_T.

2.2. Base-Collector Space Charge Region

With low current density, the BC SCR transit time is given by

$$\tau_{BC} = \frac{w_{BC}}{2v_c}, \tag{4}$$

where w_{BC} is the voltage-dependent width of the BC SCR and v_C is average field-dependent carrier velocity. When the collector is fully depleted over the width w_C, the transit time can be rewritten as

$$\begin{cases} \tau_{BC} = \tau_{BCP}\dfrac{C_{jCiP}}{C_{jCi}} \\ \tau_{BCP} = \dfrac{w_C}{2v_c} \end{cases}, \tag{5}$$

where τ_{BCP} is the punch-through transit time and C_{jCiP} is the fully depleted capacitance. (With high current density, the transit time in this region is so complicated that it is not useful in this linear model.)

2.3. Neutral Base Region

In the low-current-density region, the Kirk effect would not happen, and the base transit time can be considered as

$$\tau_{Bf} = \frac{dQ_{nB}}{di_T} = \tau_{Bfd} + \tau_{Bfv} = \frac{w_B^2}{\mu_{nB}V_T}\frac{(\zeta - 1)e^{\zeta} + 1}{\zeta^2 e^{\zeta}} + \frac{w_B}{v_c}\frac{e^{\zeta} - 1}{e^{\zeta}\zeta}, \tag{6}$$

where Q_{nB} is the minority carrier stored in the neutral base region, w_B is the neutral base width, μ_{nB} is the average base charge mobility, ζ is the drift factor, and v_C is the electron velocity at the end in this region. Here, τ_{Bfd} is defined as a drift/diffusion term and τ_{Bfv} is defined as a carrier jam term.

When the current density increases, the equation becomes more complicated. Under the assumption that drift factor is independent of bias, the base transit time is modified as follows:

$$\begin{cases} \tau_{Bfd} = \dfrac{w_{B0}^2}{\mu_{nB}V_T}\dfrac{(\zeta - 1)e^{\zeta} + 1}{\zeta^2 e^{\zeta}}[1 - k_b(c - 1)]^2 \\ \tau_{Bfv} = \dfrac{w_{B0}}{v_s}\dfrac{e^{\zeta} - 1}{e^{\zeta}\zeta}\left(1 + \dfrac{1}{u}\right) \end{cases}, \tag{7}$$

where k_b is a constant, $w_{B0} = w_B(v_{BCi} = 0)$, and u is the normalized electric field at the BC junction.

2.4. Base-Emitter Space Charge Region

In the BE SCR, the transit time is derived as follows:

$$\tau_{BE} = \frac{qA_E w_{BE} n_i \exp\left(\dfrac{v_{BEi}}{2V_T}\right)}{g_m \cdot PE} \propto \frac{1}{\sqrt{I_C}} \tag{8}$$

where g_m is the forward transconductance, PE is the built-in voltage of the BE junction, w_{BE} is the width of the BE SCR, and n_i is the average effective intrinsic carrier density within w_{BE}.

From the relation, $\tau_{BE} \propto I_C^{-1/2}$, we know that the transit time drops with high current density.

2.5. Neutral Collector Region

In this region, the storage time is given as

$$\tau_{pC} = \frac{dQ_{pC}}{di_C} = \frac{w_C^2}{4\mu_{nC0}V_T}\left[\frac{i + \sqrt{i^2 + a_{hc}}}{1 + \sqrt{1^2 + a_{hc}}}\right]^2\left[1 + \frac{2I_{CK}}{I_T\sqrt{i^2 + a_{hc}}}\right], \tag{9}$$

where Q_{pC} denotes the storage holes, $i = 1 - I_{CK}/I_T$, and a_{hc} is a constant. In the low-current-density region, this transit time can be ignored.

3. COMPACT-MODEL EQUATIONS

The model of each region described in the previous section has good physics meaning. However, the model is too complicated and difficult for model parameter extraction in a large-signal model. Hence, we introduce a compact model in this section. In addition, a new time constant is added in the transit time for fitting the measurement results accurately, especially in the low- and medium-current regimes.

3.1. Low Current Density Region

From the previous section, the transit time with low current density includes a drift/diffusion time τ_{Bfd}, a carrier jam time τ_{Bfv}, the BC

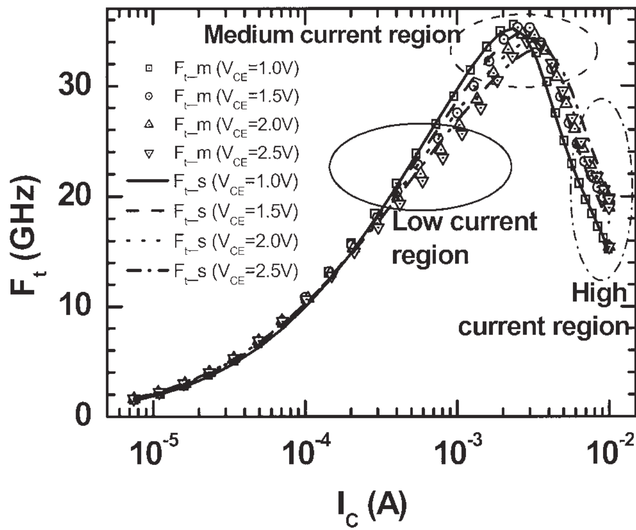

Figure 3 Measured transit-time frequency vs. collector current for various V_{CE} values and the fitting curves of the modified HICUM model

SCR transit time τ_{BC}, an electron storage time τ_{Ef}, and the BE SCR transit time τ_{BE}. Under the assumption that $I_T = I_C \ll 1$ and $\tau_{Bfd0} k_b^2 (c - 1)^2$ is ignored, the transit time can be rewritten as

$$\begin{aligned} \tau_{f0} &= \tau_{Bfd} + \tau_{Bfv} + \tau_{BC} + \tau_{Ef} + \tau_{BE} \\ &= \tau_0 + \left[\tau_{BCP} \frac{C_{jciP}}{C_{jci0}} - 2\tau_{Bfd0} k_b \right] (c - 1) + \tau_{Bfvl} \left[\frac{u_0}{u} - 1 \right] \\ &\doteq \tau_0 + \Delta\tau_{0h}(c - 1) + \tau_{Bfvl} \left[\frac{1}{c} - 1 \right]. \end{aligned} \quad (10)$$

However, this model is inaccurate for GaInP/GaAs HBT technology. Because the base doping is higher than the emitter doping in the GaAs HBT, the condition is different from that in [4]; we induce the term $\chi_{BE0}/\sqrt{i_T}$ to fit the measurement data precisely. Thus, the transit-time model becomes

$$\tau'_{f0} = \tau_{f0} + \frac{\chi_{BE0}}{\sqrt{i_T}} = \tau_0 + \Delta\tau_{0h}(c - 1) + \tau_{Bfvl} \left[\frac{1}{c} - 1 \right] + \frac{\chi_{BE0}}{\sqrt{i_T}}, \quad (11)$$

where χ_{BE0} is a constant about 5.5e-14. In Eq. (11), the parameter $\tau_0 = \tau_{Ef0} + \tau_{Bfd0} + \tau_{Bfv0} + \tau_{BCP}(C_{jCiP}/C_{jCi0})$ is the transit time with $V_{BCi} = 0$, the parameter $\Delta\tau_{0h}$ represents that the variation of the transit-time results from the variation of BC depletion width, the parameter τ_{Bfvl} stands for terms associated with carrier mobility, and the final parameter χ_{BE0} is the adjustment for fitting the curve at the low current region.

3.2. Medium/High Current Density Region

In this region, $\Delta\tau_{Ef}$ and $\Delta\tau_{fh}$ should be included. The term $\Delta\tau_{Ef}$ resulting from τ_{Ef} is written as

$$\Delta\tau_{Ef} = \tau_{Ef0}(i_T/I_{CK})^{g_{\tau E}}, \quad (12)$$

and the term $\Delta\tau_{fh}$ resulting from τ_{Bf} and τ_{pC} is represented as

$$\begin{cases} \Delta\tau_{fh} = \tau_{hcs} \left[\dfrac{i + \sqrt{i^2 + a_{hc}}}{1 + \sqrt{1^2 + a_{hc}}} \right]^2 \left[1 + \dfrac{2I_{CK}}{i_T \sqrt{i^2 + a_{hc}}} \right] \\ \tau_{hcs} = \tau_{Bfvs} + \tau_{pCs} = \dfrac{w_{Bm} w_C}{2\mu_{nC0} V_T} \dfrac{e^{\zeta}\zeta}{e^{\zeta} - 1} + \dfrac{w_C^2}{4\mu_{nC0} V_T} \end{cases}. \quad (13)$$

Here, τ_{Ef0}, $g_{\tau E}$, τ_{hcs}, and a_{hc} are extraction parameters.

Therefore, we obtain a compact model with parameters τ_0, $\Delta\tau_{0h}$, τ_{Bfvl}, χ_{BE0}, τ_{Ef0}, $g_{\tau E}$, τ_{hcs}, and a_{hc}.

4. MODEL FITTING AND RESULTS

In this section, our transit-time model is compared with the VBIC model in terms of transit-time frequency versus bias (I_C, V_{CE}). Here, the device is the npn 2×4 μm HBT device.

The formulas (11), (12), and (13) are used for parameter fitting. First of all, the extraction with low current density was performed, with τ_0 the initial value obtained from the curve close to $v_{BCi} = 0$. Then $\Delta\tau_{0h}$ was obtained by fitting various curves with V_{CE} as parameters. τ_{Bfvl} and χ_{BE0} were obtained using the optimization method. From some known process parameters, we can set the initial values as follows:

$$\begin{cases} r_{Ci0} = \dfrac{w_C}{qA_E \mu_{nC0} N_C} \approx 75\Omega \\ V_{PT} \approx 2V \\ E_{\lim} = \dfrac{V_{\lim}}{w_c} = \dfrac{v_s}{\mu_{nC0}} \Rightarrow V_{\lim} = \dfrac{v_s}{\mu_{nC0}} w_c \approx 0.2 \text{ V} \end{cases}. \quad (14)$$

All the parameters are obtained through optimization fitting and the result is shown in Figure 3 and Table 2. Obviously, the fitting curve is very close to the measured one. The model developed here is better than the VBIC model, especially in the low-current and medium-current regimes. Moreover, the modeled *ft* decreases as V_{CE} increases, as in the measured data.

TABLE 2 Model Parameter Values Used for the Examples Presented

Parameter	Value	Parameter	Value
τ_0 [psec]	2.6	τ_{hcs} [psec]	5
$\Delta\tau_{0h}$ [psec]	1.3	a_{hc}	0.65
τ_{Bfvl} [psec]	0.01	r_{Ci0} [Ω]	77
χ_{BE0}	5.5e-14	V_{PT}	2.5
τ_{Ef0}	0.4	$V_{\lim}$	0.34
$g_{\tau E}$	2.7	V_{CEs}	0.2

5. CONCLUSION

The conventional VBIC model does not give correct dependence between *ft* and V_{CE} and fails to describe *ft* at low and medium current regimes. A modified HICUM model suitable for the GaInP/GaAs HBT device for alleviating these problems has been demonstrated in this paper. The developed model helps with the design of accurate high-frequency integrated circuits.

ACKNOWLEDGMENTS

This work was supported by the National Science Council of Republic of China under contract nos. NSC 94-2752-E-009-001-PAE and NSC 94-2219-E-009-014, and by the Ministry of Economic Affairs under contract no. 94-EC-17-A-05-S1-020.

REFERENCES

1. S.V. Cherepko and J.C.M. Hwang, VBIC model applicability and extraction procedure for InGaP/GaAs HBT, APMC (2001), 716–721.
2. D. Berger, D. Céll, M. Schröter, M. Malorny, T. Zimmer, and B. Ardouin, HICUM parameter extraction methodology for a single transistor geometry, IEEE BTCM (2002), 116–119.
3. R.B. Nubling, N.H. Sheng, K.C. Wang, M.F. Chang, W.J. Ho, G.J. Sullivan, C.W. Farley, and P.M. Asbeck, 25-GHz HBT frequency dividers, Gallium Arsenide Integrated Circuit (GaAs IC) Symp Dig (1989), 125–128.
4. M. Schröter and T.-Y. Lee, Physics-based minority charge and transit time modeling for bipolar transistors, IEEE Trans Electron Devices 46 (1999), 288–300.

© 2006 Wiley Periodicals, Inc.

A RANK-REVEALING PRECONDITIONER FOR THE FAST INTEGRAL-EQUATION-BASED CHARACTERIZATION OF ELECTROMAGNETIC CRYSTAL DEVICES

Davy Pissoort,[1] Eric Michielssen,[2] Dries Vande Ginste,[1] and Femke Olyslager[1]

[1] Electromagnetics Group
Department of Information Technology
Ghent University
St.-Pietersnieuwstraat 41, Ghent, Belgium
[2] Radiation Laboratory
Department of Electrical Engineering and Computer Science
University of Michigan
1301 Beal Avenue
Ann Arbor, MI 48109

Received 18 October 2005

ABSTRACT: *A novel rank-revealing shielded-block preconditioner that accelerates the iterative integral-equation-based analysis of wave propagation in electromagnetic crystal (EC) devices is presented. The proposed shielded-block preconditioner exploits the bandgap character of the background electromagnetic crystal in order to achieve both rapid convergence of the iterative solver as well as a low matrix-vector multiplication cost. The versatility and computational efficiency of the shielded-block preconditioner are demonstrated by its application to the analysis of wave propagation in a defectless electromagnetic crystal along an electromagnetic crystal waveguide and out of an electromagnetic crystal horn antenna array.* © 2006 Wiley Periodicals, Inc. Microwave Opt Technol Lett 48: 783–789, 2006; Published online in Wiley InterScience (www.interscience.wiley.com). DOI 10.1002/mop.21475

Key words: *photonic crystals; preconditioning; rank-revealing decomposition*

1. INTRODUCTION

This paper presents a rank-revealing preconditioner that allows the fast integral-equation-based characterization of finite 2D electromagnetic crystal (EC) devices [1]. The ECs studied here comprise periodic constellations of parallel homogeneous dielectric/magnetic circular cylinders residing in a homogeneous background. Infinite and defectless ECs exhibit so-called electromagnetic bandgaps, namely, frequency ranges throughout which no fields are allowed to propagate. EC devices, including (bended) waveguides [2, 3], multiplexers [4–6], super-prisms [7], and horn antennas [8, 9] can be created by removing/adding cylinders from/to finite though otherwise defectless ECs.

In the past, field propagation in finite EC devices often has been analyzed using multiple scattering techniques (MSTs) [10, 11], which solve boundary integral equations in terms of total electric and/or magnetic fields tangential to the EC cylinders' surfaces. Often, these MSTs exploit the cylinders' circular nature by expanding total fields in terms of angular Fourier series of Bessel/Hankel functions. Such MSTs achieve high accuracy with only a few unknowns per cylinder. The principal disadvantage of MSTs is that they require the solution of dense linear systems of equations whose dimensions scale linearly with the number of cylinders, denoted as N_c. The cost of solving these systems directly and iteratively scales as $O(N_c^3)$ and $O(pN_c^2)$, respectively; here, p denotes the number of iterations required. These costs are prohibitive, as EC devices almost invariably are electromagnetically large while containing near-resonant components, thereby leading to large N_c and p and necessitating the use of effectively preconditioned iterative solvers relying on fast matrix-vector multiplication schemes [12].

This paper describes a left shielded-block preconditioner that permits the fast iterative integral-equation-based analysis of field propagation in finite EC devices. Starting from a dense interaction matrix obtained by applying the MST to the analysis of an EC device, the proposed preconditioner is constructed as follows. First, the EC under study is subdivided into a number of physically nonoverlapping blocks of cylinders of roughly equal size. Second, each block of EC cylinders thus obtained is encased in a shield of preset thickness comprising (available) cylinders drawn from neighboring blocks. Third, for each block, the block plus shield self-interaction matrix is inverted and all the rows of the resulting matrix pointing to field variables inside the shield are discarded. Fourth and finally, the shielded-block preconditioner is applied by left-multiplying the original MST global interaction matrix and excitation vector through the collection of all restricted inverses. The inclusion of a shield while forming the preconditioner has two effects. First, it improves the quality of the preconditioner beyond that of a classical (block) diagonal one (which, upon applying the above-outlined procedure, would result in the use of a zero thickness shield), thereby reducing the iteration counts. Second, it (approximately) reduces the interaction rank of different blocks to that intended for proper device operation, thereby allowing nonself group interactions to be accounted for using low-rank matrix-vector product methods. We note that the use of physical-shielding concepts to construct preconditioners that accelerate the convergence of integral-equation solvers pertinent to the analysis of electromagnetic phenomena is not new; ideas similar to those presented here have been used, for example, to accelerate capacitance extraction codes [13]. However, the application of such techniques to the analysis of wave propagation in EC devices yields dramatic improvement over classical preconditioners because they optimally exploit the bandgap character of the underlying EC while maintaining flexibility with regard to the nature of the devices analyzed, that is, without reverting to the use of so-called periodic EC Green functions [14]. The proposed scheme is in contrast to other fast preconditioned integral equation solvers for characterizing EC devices in that it simultaneously addresses preconditioning and acceleration needs.

This paper is organized as follows. Section 2 describes a classical MST for analyzing finite EC devices comprising dielectric/magnetic circular cylinders immersed in a homogeneous background. Section 3 details the construction of the proposed shielded-block preconditioner and demonstrates its effectiveness, both in terms of reducing the iteration counts of MST solvers and accelerating their matrix-vector products. Finally, section 4 elucidates